RSC Advances

PAPER

View Article Online
View Journal | View Issue

Cite this: *RSC Adv.*, 2014, **4**, 37400

Synthesis of glycopolymers at various pendant spacer lengths of glucose moiety and their effects on adhesion, viability and proliferation of osteoblast cells†

Mummuluri Trinadh,[a] Govindaraj Kannan,[b] Tota Rajasekhar,[a] Annadanam V. Sesha Sainath*[a] and Marshal Dhayal*[b]

Received 7th June 2014
Accepted 30th July 2014

DOI: 10.1039/c4ra05436a

www.rsc.org/advances

Multivalent glycopolymers containing three different glucose pendant spacer lengths in the polymer backbone having various weight percentages of covalently bonded glucose moieties were obtained by the deacetylation of acetylated polymers synthesized *via* reversible addition-fragmentation chain transfer (RAFT) process. This allowed us to control the packing density of the glucose moieties in one unit of the glycopolymer. The biological responses of these macromolecules in terms of cytotoxicity of glucose moieties at various spacer lengths and concentrations were investigated without perturbing the intrinsic chemical nature of functional moiety by employing *in vitro* osteoblast cells. Osteoblast cell adhesion, viability and proliferation response with synthesized glycopolymers revealed that the higher glycopolymer concentration tolerance limit was associated with an increase in pendant spacer length of glucose moiety in the glycopolymer.

1. Introduction

The unique properties of glycopolymers, which consist of a synthetic polymeric backbone and pendant glyco-moieties have been applied in clinical diagnostics, drug and gene delivery systems,[1–6] specific molecular recognition,[7–16] surface modifiers[17–19] and separation of biomolecules.[20–23] Hence, the interests of researchers have been focused on dealing with the design and development of suitable glycopolymeric materials by tailoring macromolecular chains and testing their biological performance. Well-defined glycopolymeric materials provide structural and functional support to cells/tissues due to their hydrophilic character, better biocompatibility and ability to mimic glycoproteins in the biological systems.[24–27] The carbohydrate units in glycopolymers act as ligands in a variety of biological processes and play a significant role in biomolecule recognition and determine the interaction with cells for desirable tissue growth and repair.[28–32] Moreover, glycans are specific for the regulation of certain cellular functions due to their multivalent nature and flexibility while the varying spatial distribution of glyco-moieties in glycans have advantages in developing new materials for biomedical applications.[33,34] The initial study by Schnaar *et al.* demonstrated the adhesion of chicken hepatocytes to poly(acrylamide) gels, which were derivatized with *N*-acetylglucosamine glycopolymeric coatings.[35] The fibroblast cell adhesion and proliferation on hyperbranched glycoacrylate films and glycopolymer coatings on polystyrene carrying *N*-acetylglucosamine residues were studied.[36,37] The biocompatibility of sugar-modified extracellular matrices of glycopolymers had been extensively studied in liver cells by varying carbohydrate moieties in polymeric backbone architectures.[38–42]

Synthetic glycopolymers are a useful tool, which allows the precise control of various biological functions of a cell during cell/surface interactions. The development of new methods for the synthesis of tailor-made glycopolymers, as well as glycan derivatives, has given access to targeted architectures and modifications with carbohydrate moieties.[43,44] Previously, glucose moiety containing glycopolymer (poly-[3-*O*-(4′-vinylbenzyl)-D-glucose]) was used for culturing erythrocytes and observations confirmed that the presence of reducing glucose moieties was crucial for specific cell attachment.[45,46] Despite all of these biologically important functions, there has been very little attention paid towards the use of glycopolymers having different pendant alkyl chain lengths of glucose functional moiety on polymer backbone in cell and tissue engineering.

To the best of our knowledge, the osteoblast cell adhesion, viability and proliferation with glycopolymers, consisting of

[a]*Polymers and Functional Materials Division, CSIR-Indian Institute of Chemical Technology, Hyderabad 500007, Andhra Pradesh, India. E-mail: avssainath@yahoo.com; Fax: +91 40 27160591; Tel: +91 40 27192500*

[b]*Clinical Research Facility, CSIR-Center for Cellular and Molecular Biology, Hyderabad 500007, Andhra Pradesh, India. E-mail: marshal@ccmb.res.in*

† Electronic supplementary information (ESI) available: Detailed characterisation of glycopolymer and cellular response of free glucose. See DOI: 10.1039/c4ra05436a

various pendant alkyl chain of glucose moiety has not been examined yet. However, previously, osteoblast cell adhesion to various implant materials, such as metal oxides, bioinert metals, metal alloys, bioceramics, synthetic polymers and composites, has been extensively studied.[47–54] Formerly, poly(pentafluorostyrene) based glycopolymer coated substrates were used to study the attachment of 3T3 fibroblasts and MC3T3-E1 preosteoblasts.[55] It was expected that the studies of osteoblast cell response at various concentrations of glycopolymers having different pendant alkyl chain lengths of glucose functional moieties on acrylate macromolecular chain could help in designing bone implant coatings that modulate cell adhesion and proliferation within the multicellular environment of the human body. Thus, the study of osteoblast cell interactions with glycopolymers is of great interest for hard tissue engineering and understanding bone formation process.[56]

Here we used the RAFT process for the syntheses of glycopolymers containing three different glucose pendant alkyl chain lengths in the polymer backbone. The RAFT process is a commonly used and reliable method for the synthesis of glycopolymers to achieve controlled macromolecular architecture from a wide range of functional monomers.[57–59] In this paper, we report the usefulness of functional moiety with different pendant alkyl chain lengths in glycopolymers to control the response of different cellular functions such as adhesion, viability and proliferation of mouse osteoblast (MC3T3) cells *in vitro*.

2. Experimental

2.1 Materials

D-Glucose anhydrous (Fisher Scientific, Qualigens), acetic anhydride and sodium acetate (Sisco Research Laboratories Pvt. Ltd.), benzylamine (Finar Chemicals Limited), methyl ethyl ketone (MEK), acryloyl chloride, triethylamine (Et_3N) and azobisisobutyronitrile (AIBN) (Avra Synthesis Pvt. Ltd.), 1,4-butanediol, 1,6-hexanediol, boron trifluoride diethyl etherate ($BF_3 \cdot Et_2O$) and 2-cyano-2-propyldodecyltrithiocarbonate (CPDTC) (Sigma-Aldrich) and molecular sieves 4 Å (SDFCL, s d fine-chem Limited) were used as received. Dichloromethane (DCM) (Finar Chemicals Ltd.) was dried over calcium hydride by stirring overnight and distillation. Tetrahydrofuran (THF) (Finar Chemicals Limited) was distilled over sodium wire with benzophenone under a nitrogen atmosphere. The osteoblast cells (MC3T3) were obtained from American type culture collection (ATCC), USA, and their subclones were maintained in a complete medium (CM). The CM was made of fresh α-minimum essential medium (MEM) (Invitrogen, USA) having 10% fetal bovine serum (FBS) (Invitrogen, USA) and 100 U mL^{-1} penicillin, 50 μg mL^{-1} streptomycin and 50 μg mL^{-1} gentamycin (Invitrogen, USA). The cells were sub-cultured using trypsin-ethylenediaminetetraacetic acid (EDTA) (Invitrogen, USA).

2.2 Preparation of 1,2,3,4,6-penta-*O*-acetyl-D-glucopyranoside (PAGP)

Well-ground mixture of 20 g (0.11 mol) of D-glucose and 25 g (0.304 mol) of sodium acetate was taken in a 500 mL two-necked, round-bottomed flask, followed by 150 mL of acetic anhydride and refluxed for 4 h. After the solution became clear, it was poured into a conical flask which contained crushed ice. The generated crystals were filtered with a Büchner funnel and dried. Yield: 75%. M.p. 113–115 °C. ^{1}H NMR ($CDCl_3$, 300 MHz): δ 5.73 (d, $j = 7.93$ Hz, 1H), 5.26 (m, 1H), 5.14 (t, $j = 9.06$, 7.55 Hz, 2H), 4.30 (m, 1H), 4.11 (d, $j = 11.71$ Hz, 1H), 3.86 (d, $j = 7.18$ Hz, 1H) and 2.09–2.02 (m, 15H). ESI-MS: m/z: 413 $(M + Na)^+$. IR (KBr, cm^{-1}): ν 2969 (–CH–), 1746 (–O–*C*=*O*–), 1375 (–O–C–, ester) and 1226 (–C–O–C–).

2.3 Preparation of 2,3,4,6-tetra-*O*-acetyl-D-glucopyranoside (TAGP)

A solution of PAGP (5.0 g, 0.0128 mol) and benzylamine (2.1 mL, 0.0192 mol) in 30 mL of THF was taken in a 100 mL two-necked, round-bottomed flask and stirred overnight at room temperature.[60] The mixture was diluted with cold water and extracted with chloroform (3 × 200 mL). The extracted layer was successively washed with ice cold dilute HCl solution, saturated $NaHCO_3$ solution, saturated NaCl solution and water. The mixture was dried over anhydrous Na_2SO_4 and concentrated in vacuum. The residue was purified by column chromatography with ethyl acetate and *n*-hexane (2/3, v/v) mixture to afford 3.5 g of TAGP, which is a viscous liquid. Yield: 80%. ^{1}H NMR ($CDCl_3$, 300 MHz): δ 5.55 (t, $j = 9.44$ Hz, 1H), 5.43 (s, 1H), 5.07 (t, $j = 9.06$ Hz, 2H), 4.87 (d, $j = 9.44$ Hz, 1H), 4.37 (s, 1H), 4.24 (m, 1H), 4.08 (s, 1H) and 2.17–2.01 (m, 12H). ESI-MS: m/z: 371 $(M + Na)^+$. IR (KBr, cm^{-1}): ν 3328 (–OH), 2956 (–CH–), 1750 (–O–*C*=*O*–), 1432, 1370 (–O–C–, ester) and 1231 (–C–O–C–).

2.4 Synthesis of 4-hydroxybutyl acrylate (HBA)

HBA was prepared as reported in literature.[61] 1,4-Butanediol (26.9 g, 0.299 mol) was reacted with acryloylchloride (6.92 g, 0.0765 mol) in the presence of triethylamine (10.9 g, 0.108 mol). The obtained mixture was purified by column chromatography using hexane/ethyl acetate (v/v, 1 : 1) as eluent. Note that HBA was liquid in nature. ^{1}H NMR ($CDCl_3$, 300 MHz): δ 6.40 (d, $j = 17.18$ Hz, 1H), 6.20–6.03 (m, 1H), 5.82 (d, $j = 10.39$ Hz, 1H), 4.19 (m, 2H), 3.67 (m, 2H) and 1.88–1.54 (m, 4H). ESI-MS: m/z: 145 $(M + H)^+$. IR (KBr, cm^{-1}): ν 3425 (–OH), 2951 (–CH–), 1723 (–O–*C*=*O*–), 1410, 1370 (–O–C–, ester) and 1194 (–C–O–C–).

2.5 Preparation of 6′-hydroxyhexyl-2,3,4,6-tetra-*O*-acetyl-D-glucopyranoside (HHTAGP)

A solution of PAGP (10 g, 0.026 mol) in dichloromethane (80 mL) was stirred for 2 h with molecular sieves (4 g, 0.4 mm) under nitrogen atmosphere.[62] Then, $BF_3 \cdot Et_2O$ (6.5 mL, 0.051 mol) was subsequently added to the mixture, immediately followed by 1,6-hexanediol (3.32 g (0.028 mol) in 15 mL dichloromethane). After 10 days, the mixture was poured into saturated $NaHCO_3$ solution (100 mL). The organic layer was separated and the aqueous phase was extracted with dichloromethane 3 times, each time with 40 mL of dichloromethane. The total collected organic layer was washed twice with water, each time with 40 mL of water. Dichloromethane was evaporated under vacuum and the resulting syrup was purified by column

chromatography (hexane/ethyl acetate, 7 : 3 (v/v)). Note that HHTAGP was a viscous liquid. Yield: 40%. ^{1}H NMR ($CDCl_3$, 300 MHz): δ 5.55–5.32 (d, j = 32.86 Hz, 1H), 5.15–4.92 (m, 2H), 4.87–4.72 (d, j = 11.71 Hz, 1H), 4.36–4.16 (d, j = 11.71 Hz, 1H), 4.14–3.88 (m, 4H), 3.76–3.61 (broad s, 1H), 3.52–3.34 (broad s, 1H), 2.24–1.88 (m, 12H) and 1.73–1.15 (m, 8H). ESI-MS: m/z: 471 $(M + Na)^+$. IR (KBr, cm^{-1}): ν 3328 (–OH), 2956 (–CH–), 1750 (–O–*C*=*O*–), 1432, 1370 (–O–C–, ester) and 1231 (–C–O–C–).

2.6 Preparation of glycoacrylates, acryl-2,3,4,6-tetra-*O*-acetyl-D-glucopyranoside (ATAGP) and 6′-(acryloxy)hexyl-2,3,4,6-tetra-*O*-acetyl-D-glucopyranoside (AHTAGP)

ATAGP and AHTAGP were synthesized according to a typical standard procedure as follows. A solution of TAGP (18 g, 0.0517 mol) in 180 mL of MEK and 14.39 mL (0.1035 mol) of Et_3N was taken in a 500 mL two-necked, round-bottomed flask equipped with a magnetic stirrer and placed in an ice bath. Acryloyl chloride (5.55 mL (0.0568 mol) in 25 mL of MEK) was added drop by drop with constant stirring without raising the temperature above 0 °C. The reaction mixture was stirred for a period of 5 h after removing from the ice bath. The quaternary ammonium salt (precipitate) was filtered. The supernatant was washed with cold distilled water and dried with anhydrous Na_2SO_4. ATAGP was isolated by evaporating the solvent and purified by column chromatography technique. Yield: 75%. M.p. 59-62 °C. ^{1}H NMR ($CDCl_3$, 300 MHz): δ 6.59–6.35 (m, 1H), 6.25–6.03 (m, 1H), 6.01–5.90 (t, j = 10.20 Hz, 1H), 5.81–5.71 (d, j = 7.93 Hz, 1H), 5.53–5.41 (t, j = 9.82 Hz, 1H), 5.30–5.06 (m, 1H), 4.33–4.19 (m, 1H), 4.17–3.99 (d, j = 3.40 Hz, 1H), 3.92–3.79 (d, j = 7.93 Hz, 1H) and 2.12–1.87 (m, 12H). ^{13}C NMR ($CDCl_3$, 75 MHz): δ 20.24, 20.37, 20.41, 20.51, 61.31, 67.68, 67.80, 69.10, 69.76, 70.05, 72.55, 72.61, 89.18, 91.81, 132.92, 133.34, 163.61, 169.07, 169.23, 169.53, 169.89, 170.0 and 170.42. ESI-MS: m/z: 425 $(M + Na)^+$. IR (KBr, cm^{-1}): ν 2963 (–CH–), 1750 (–O–*C*=*O*–), 1634 (–C=C–), 1409, 1370 (–O–C–, ester) and 1221 (–C–O–C–). AHTAGP: yield: 75%, viscous liquid. ^{1}H NMR ($CDCl_3$, 500 MHz): δ 6.47–6.36 (d, j = 17.0 Hz, 1H), 6.19–6.05 (m, 1H), 5.82–5.78 (d, j = 10.58 Hz, 1H), 5.27–5.15 (t, j = 9.44 Hz, 1H), 5.15–5.04 (m, 1H), 5.04–4.92 (m, 1H), 4.52–4.46 (d, j = 7.93 Hz, 1H), 4.32–4.22 (m, 4H), 4.20–4.08 (d, j = 7.18 Hz, 1H), 3.94–3.81 (m, 1H), 3.76–3.64 (d, j = 9.44 Hz, 1H), 3.55–3.41 (m, 1H), 2.15–2.19 (m, 12H), 1.73–1.50 (m, 4H) and 1.45–1.29 (s, 4H). ^{13}C NMR ($CDCl_3$, 75 MHz): δ 20.35, 20.47, 61.27, 67.64, 69.06, 69.67, 70.01, 72.47, 72.54, 91.74, 126.87, 133.29, 163.56, 169.01, 169.18, 169.83 and 170.34. ESI-MS: m/z: 525 $(M + Na)^+$. IR (KBr, cm^{-1}): ν 2962 (–CH–), 1745 (–O–*C*=*O*–), 1633 (–C=C–), 1409, 1376 (–O–C–, ester) and 1230 (–C–O–C–).

2.7 Preparation of 4′-(acryloxy)butyl-2,3,4,6-tetra-*O*-acetyl-D-glucopyranoside (ABTAGP)

PAGP (10 g, 0.026 mol) and 4-hydroxybutyl acrylate (3.32 g, 0.023 mol) were dissolved in 70 mL of DCM and $BF_3 \cdot Et_2O$ (10.92 g, 0.077 mol) was subsequently added *via* a syringe. Note that the mixture was sonicated for 45 min. The reaction mixture was washed with saturated brine solution and the organic layer was dried over $MgSO_4$. After removing the solvent under reduced pressure, the yellow syrup was purified by flash column chromatography using hexane and ethyl acetate mixture (7 : 3, v/v). Yield: 45%. ^{1}H-NMR ($CDCl_3$, 500 MHz): δ 6.47–6.40 (dd, j = 1.07 Hz, 1H), 6.16–6.06 (m, 1H), 5.93–5.88 (dd, j = 1.07 Hz, 1H), 5.58–5.51 (t, j = 9.77 Hz, 1H), 5.15–5.06 (m, 2H), 4.96–4.91 (dd, j = 3.66 Hz, 1H), 4.31–4.17 (m, 2H), 4.16–3.99 (m, 4H), 3.77–3.69 (m, 1H), 3.51–3.39 (m 1H), 2.09–1.97 (m, 12H), 1.81–1.53 (m, 2H) and 1.31–1.20 (m, 2H). ^{13}C NMR ($CDCl_3$, 75 MHz): δ 20.59, 20.91, 25.27, 25.80, 29.64, 61.37, 61.96, 63.95, 67.24, 67.78, 68.10, 68.46, 69.21, 69.82, 70.07, 70.53, 70.96, 72.68, 95.70, 127.37, 132.41, 165.09, 169.56, 170.17, 170.63 and 171. IR (KBr, cm^{-1}): ν 2949 (–CH–), 1750 (–O–*C*=*O*–), 1634 (–C=C–), 1409, 1369 (–O–C–, ester) and 1227 (–C–O–C–).

2.8 Polymerization

All the monomers, *i.e.* ATAGP, AHTAGP and ABTAGP, were polymerized *via* the RAFT method. A typical ATAGP polymerization procedure is as follows. A mixture of acryl-2,3,4,6-tetra-*O*-acetyl-D-glucopyranoside (1.7 g, 0.0042 mol), AIBN (18 mg, 0.00012 mol) and RAFT agent, CPDTC (58 mg, 0.00016 mol) in 20 mL of THF was deoxygenated by freeze and thaw cycle for three times. Then, the flask was sealed and heated to 80 °C with stirring. It was allowed to polymerize for 30 h. After that, the polymerization was stopped by the addition of 0.5 mL of methanol and exposed to air. The polymer was isolated by precipitating in cold methanol twice and once in 30% ethyl acetate in hexane. The yield of poly(acryl-2,3,4,6-tetra-*O*-acetyl-D-glucopyranoside) (P(ATAGP)) was about 55%. P(ATAGP): ^{1}H NMR ($CDCl_3$, 300 MHz): δ 6.40–6.16, 5.80–5.57, 5.52–5.35, 5.34–5.20, 5.19–4.68, 4.51–4.18, 4.17–3.98, 3.96–3.72, 2.73–2.24, 2.21–1.82, 1.79–1.06 and 0.90–0.75. ^{13}C NMR ($CDCl_3$, 75 MHz): δ 67.73, 69.77, 70.12, 72.70, 89.17, 89.65, 169.23, 169.32, 169.98, 170.47 and 170.56. IR (KBr, cm^{-1}): ν 2962 (–CH–), 1756 (–O–*C*=*O*–), 1634 (–C=S–), 1439, 1374 (–O–C–, ester) and 1226 (–C–O–C–). Poly(4′-(acryloxy)butyl-2,3,4,6-tetra-*O*-acetyl-D-glucopyranoside) (P(ABTAGP)): yield: 46%. ^{1}H NMR ($CDCl_3$, 300 MHz): δ 6.47–6.16, 5.89–5.56, 5.53–5.37, 5.37–5.25, 5.25–4.90, 4.56–4.23, 4.20–4.01, 3.98–3.82, 2.85–2.29, 2.26–1.78, 1.56–0.95 and 0.92–0.82. ^{13}C NMR ($CDCl_3$, 75 MHz): δ 20.68, 61.09, 65.11, 67.64, 69.24, 69.62, 72.35, 72.58, 72.67, 89.17, 169.00, 169.17, 169.37, 169.90 and 169.98. IR (KBr, cm^{-1}): ν 2962 (–CH–), 1755 (–O–*C*=*O*–), 1635 (–C=S–), 1437, 1371 (–O–C–, ester) and 1226 (–C–O–C–). Poly(6′-(acryloxy)hexyl-2,3,4,6-tetra-*O*-acetyl-D-glucopyranoside) (P(AHTAGP)): yield: 68%. ^{1}H NMR ($CDCl_3$, 300 MHz): δ 6.40–6.24, 5.84–5.59, 5.53–5.37, 5.37–5.21, 5.21–4.95, 4.48–4.20, 4.20–4.03, 3.99–3.79, 3.76–3.54, 2.74–2.25, 2.19–1.94, 1.93–1.92 and 0.93–0.81. ^{13}C NMR ($CDCl_3$, 75 MHz): δ 20.45, 68.26–67.27, 70.46–69.60, 72.61, 91.75, 169.11, 169.32, 169.30, 170.51 and 170.61. IR (KBr, cm^{-1}): ν 2963 (–CH–), 1756 (–O–*C*=*O*–), 1634 (–C=S–), 1437, 1372 (–O–C–, ester) and 1226 (–C–O–C–).

2.9 Deacetylation of pendant 2,3,4,6-tetra-*O*-acetyl-D-glucopyranoside moieties

The deacetylated polymers, poly(acryl-D-glucopyranoside) (**GP1**), poly(4′-(acryloxy)butyl-D-glucopyranoside) (**GP2**) and poly(6′-

(acryloxy)hexyl-D-glucopyranoside) (**GP3**), were synthesized according to a typical procedure as follows.

The P(ATAGP) (200 mg) was dissolved in anhydrous methanol and chloroform (2 : 1) (total volume: 10 mL) and stirred under nitrogen atmosphere. A solution of NaOMe (101 mg) in anhydrous methanol (2 mL) was added through a syringe and the reaction mixture was left stirring for 90 min. Then, the solvent was removed by vacuum evaporation and neutralized with 2 M HCl solution by stirring overnight. After that, the solution was passed through basic alumina to neutralize the solution. Excess water was removed by lyophilisation, and the polymer was recovered as a white powder by precipitation in excess acetone. **GP1**: IR (KBr, cm^{-1}): ν 3425 (–OH–), 2927 (–CH–), 1735 (–O–*C*=*O*–), 2200 (–CN) and 1628 (–C=S–). **GP2**: IR (KBr, cm^{-1}): ν 3416 (–OH–), 2962 (–CH–), 1750 (–O–*C*=*O*–), 2200 (–CN) and 1620 (–C=S–). **GP3**: IR (KBr, cm^{-1}): ν 3425 (–OH), 2927 (–CH–), 1755 (–O–*C*=*O*–), 1635 (–C=S–), 1430, 1383 (–O–C–, ester) and 1239 (–C–O–C–).

2.10 Estimation of weight percentage of covalently bonded glucose moiety in glycopolymer

Covalently bonded glucose moiety in glycopolymer was calculated to determine their packing density in one unit of glycopolymer. The degree of polymerization (D_p) of glycopolymer was estimated using eqn (1).

$$D_p = \left[\frac{\{G_p(M_w) - 345\}}{M(F_w)}\right] \quad (1)$$

where $G_p(M_w)$: molecular weight of deacetylated glycopolymer by ^1H NMR, $M(F_w)$: formula weight for deacetylated monomer and 345 is a constant, representing the molecular weight of terminal ends of macromolecular chain generated by RAFT agent. Hence, glucose moiety (G_M) wt% was calculated using eqn (2).

$$G_M(wt\%) = 100 \times D_p \left[\frac{G_M(F_w)}{G_p(M_w)}\right] \quad (2)$$

where $G_M(F_w)$ is glucose moiety formula weight. All weight percentages of covalently bonded glucose moiety on three glycopolymers were calculated using the above equations.

2.11 *In vitro* cell assays

Cell culture and statistical analysis. The adherent osteoblast cells (MC3T3) were maintained in CM at 37 °C in 5% CO_2. The CM was prepared using α-MEM medium, supplemented with 10% FBS and 100 U mL^{-1} penicillin, 50 μg mL^{-1} streptomycin and 50 μg mL^{-1} gentamycin. The cells were sub-cultured after reaching 80% confluency using trypsin-EDTA. In a 96-well plate, 10^4 cells were plated in each well and different concentrations of glycopolymer were added to the cells. The stock solution of different concentrations of all three glycopolymers were prepared in phosphate buffered saline (PBS) and sterilized by autoclaving at 121.5 °C for 20 min. Final concentrations of the glycopolymer ranging from 1 nM to 10 000 μM were achieved by adding 4 μL of stock solution of different desired concentrations in 96 μL of CM for each set of experiments. Separate stock solutions of the glycopolymers were prepared for each concentration, and it was in such a manner that only 4 μL of solution was added to achieve all the desired final concentrations. All cell culture experiments were performed in triplicates with cells not exceeding ten passages post revival. The statistical analysis for *in vitro* cell assay was performed based on three experiments for each condition in which a minimum of three samples were used. Microsoft Excel software was used for calculating mean and standard deviation values for all assays.

Cell adhesion assay. This assay was carried out by plating similar number of cells in the plastic tissue culture plate wells. After 4 h, non-adherent cells were washed off and 10 μL of 2 mg mL^{-1} MTT (3-(4,5-dimethylthiazol-2-yl)-2,5-diphenyltetrazolium bromide) was added to the remaining cells of each condition, followed by incubation at 37 °C and 5% CO_2 for 4 h. After removing CM, the reaction was stopped by adding dimethylsulfoxide and read at 595 nm by ELISA reader.

Cell viability assay. The assay was performed by plating similar number of cells of all conditions in triplicates and incubated. After 24 h of incubation, MTT assay was performed as described above to calculate the percentage of cell viability.

Cell proliferation assay. The assay was performed by plating similar number of cells of all conditions in triplicates and incubated at dissimilar time periods, namely, 4, 24, 48 and 72 h. At the specified time periods cell number at each concentration was calculated by MTT assay as described above.

Immunofluoresence staining. Different concentrations of glycopolymer were added to the cells plated in a 6-well plate and incubated for 24 h. After this, the cells were fixed with 4% formaldehyde (Sigma, USA) for 5–6 min. Cells were washed with PBS for 3 times and permeabilization was performed with 0.1% Triton X-100 for 5–6 min after washing with PBS for 3 times. Blocking was performed with 3% bovine serum albumin (BSA, Sigma) for 1 h, and cells were washed with PBS once. Rodamine-phalloidin (Molecular Probes, USA) diluted in 1% BSA to 1 : 200 ratio was added on to the cells and incubated for 1 h. Finally, cells were washed once with PBS and mounted using fluoroshield 4′,6-diamidino-2-phenylindole (DAPI) (Sigma, USA). Cells were imaged with fluorescent microscope (Axio Imager.Z1, Carl Zeiss, Jena Germany). Integrin α5 and talin co-staining was carried out as follows: after 24 h, cells on the above substrates were fixed in 4% paraformaldehyde for 10 min at room temperature, permeabilized with 0.1% Triton-X-100 for 10 min and blocked with 3% BSA for 30 min. The cells were treated with rabbit anti-mouse integrin α5 antibody at 1 : 200 (Santa Cruz, USA) for 1 h at room temperature, followed by 1 h incubation with goat anti-rabbit FITC (fluorescein isothiocyanate) at 1 : 200 (GeneI, Bangalore, India). The same procedure and conditions were repeated for talin staining with mouse, anti-mouse talin antibody, followed by a 1 h incubation with goat anti-mouse TRITC in the dark at room temperature. Images were captured using a 40× and 63× objective using AxioVision imaging system (Zeiss, Germany).

2.12 Measurements

The FT-IR (Thermo Nicolet Nexus 670 spectrometer) spectra were recorded at a resolution of 4 cm^{-1} using KBr optics at

room temperature and a minimum of 32 scans were signal averaged. The proton nuclear magnetic resonance (^{1}H NMR) and carbon nuclear magnetic resonance (^{13}C NMR) spectra were recorded on AVANCE-300 or INOVA-500 spectrometer in $CDCl_3$ or D_2O (Aldrich) depending on the solubility of the products with tetramethylsilane as an internal standard. Mass spectra were recorded on FINNGAN LCQ Advance Max in methanol. Gel permeation chromatography (GPC) was performed by using a Shimadzu system built-in with one (300 × 7.5 mm) PLgel 5 μm 10×10^3 Å column (VARIAN) and evaporative light-scattering (PL-ELS) detector (Polymer Laboratories). The eluent was DMF with a flow rate of 0.5 mL min^{-1} at 30 °C. Calibration for detector response was gained using a single narrow PS standard (molecular weights: 550, 1480; 3950; 10 680 and 31 420 from Polymer Labs). 1 mg of polymer was dissolved in 1 mL of DMF. Values of M_n and M_w/M_n were determined using LC Solution for Windows software. CO_2 incubator was purchased from Thermo Scientific, USA. Spectrophotometric measurements of adhesion and proliferation were taken from Molecular Devices – Spectra Max – 190, USA.

3. Results and discussion

3.1 Glycopolymers characterization

The synthesized glycoacrylates, acryl-2,3,4,6-tetra-*O*-acetyl-D-glucopyranoside (ATAGP), 4′-(acryloxy)butyl-2,3,4,6-tetra-*O*-acetyl-D-glucopyranoside (ABTAGP) and 6′-(acryloxy)hexyl-2,3,4,6-tetra-*O*-acetyl-D-glucopyranoside (AHTAGP), were polymerized by RAFT process using 2-cyano-2-propyldodecyltrithiocarbonate as RAFT agent with azobisisobutyronitrile as a radical initiator to produce homopolymers, poly(acryl-2,3,4,6-tetra-*O*-acetyl-D-glucopyranoside) (poly(ATAGP)), poly(4′-(acryloxy)butyl-2,3,4,6-tetra-*O*-acetyl-D-glucopyranoside) (poly(ABTAGP)) and poly(6′-(acryloxy)hexyl-2,3,4,6-tetra-*O*-acetyl-D-glucopyranoside) (poly(AHTAGP)) with a dodecyl alkyl terminal end, respectively. The resulted polymer pendant units, 2,3,4,6-tetra-*O*-acetyl-D-glucopyranoside, were deacetylated in the presence of sodium methoxide/chloroform/methanol mixture to obtain poly(acryl-D-glucopyranoside) (**GP1**), poly-(4-(acryloxy)butyl-D-glucopyranoside) (**GP2**) and poly(6-(acryloxy)-hexyl-D-glucopyranoside) (**GP3**) glycopolymers, respectively. The structures of the polymers before and after deacetylation are shown in Scheme 1.

After deacetylation, number average molecular weights (M_n), 10 829, 9856 and 4266 g mol^{-1} for **GP1**, **GP2** and **GP3**, respectively

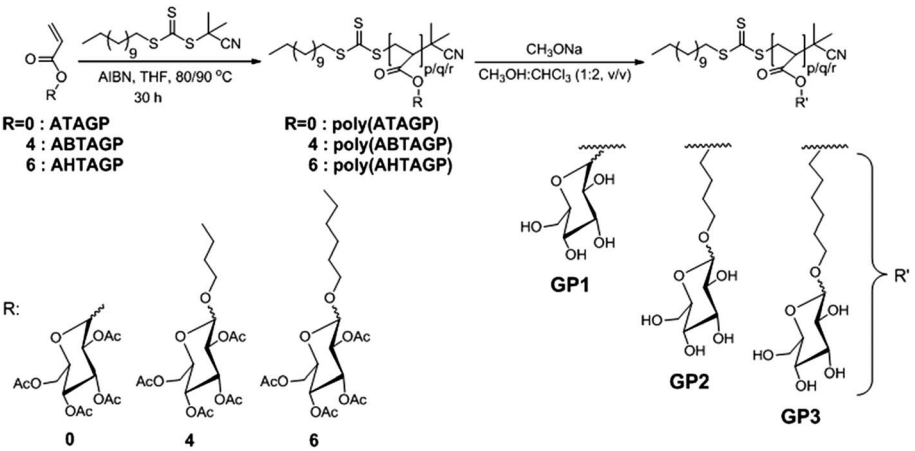

Scheme 1 Schematic representation of the syntheses of glycopolymers (0, 4 and 6 indicate spacer length) *via* the RAFT process and the deacetylation of the pendant 2,3,4,6-tetra-*O*-acetyl-D-glucopyranoside.

Table 1 Characteristics of acetylated and deacetylated glycopolymers

Acetylated				Deacetylated				
	GPC[a]				GPC[a]			
Polymer	M_n	M_w/M_n	T_g[b]/°C	Polymer	M_n	M_w/M_n	Molecular weight[c] (cal.)	T_g[b]/°C
P(ATAGP)	15 345	1.09	86	**GP1**	10 829	1.15	9880	1
P(ABTAGP)	18 450	1.13	97	**GP2**	9856	1.16	13 582	4
P(AHTAGP)	10 959	1.07	71	**GP3**	4266	1.03	7917	7

[a] In DMF at room temperature. [b] From DSC curve on second heating. [c] Molecular weight = M_w(GPC value of acetylated glycopolymer) − {[M_w (GPC) − 345] ÷ monomer molecular weight} × 168}, where 345 and 168 are the macromolecular terminal ends molecular weight and total pendant acetates molecular weights.

with M_w/M_n: ~1.15 (Table 1) were obtained by gel permeation chromatography studies in DMF with polystyrene standards. The deacetylated glycopolymers, **GP1**, **GP2** and **GP3**, which were insoluble in water prior to deacetylation, were now soluble in water. Signal integrations of the glucose moieties in pendant acetylated polymers, 2,3,4,6-tetra-*O*-acetyl, appeared at δ 1.8–2.3 ppm in ^{1}H NMR spectrum, as shown in Fig. 1a. After deacetylation, the acetyl peaks of the polymers disappeared and new signals corresponding to the OH groups of the glucose moieties[63] emerged at δ 3.8–3.92 ppm (Fig. 1b).

The FT-IR analyses of poly(ATAGP), poly(ABTAGP) and poly(AHTAGP) exhibited characteristic strong absorptions for C=O stretching centred at about 1756 cm^{-1} while the C=O stretching peaks in **GP1**, **GP2** and **GP3** shifted to 1735 cm^{-1} with lower intensities (ESI, Fig. S7 and S8†). The OH signals in **GP1**, **GP2** and **GP3** showed characteristic strong absorption centred at 3425 cm^{-1}. After deacetylation, the glass transition temperature values of the polymers were in the range of 1–7 °C, whereas acetylated polymers showed 71–97 °C as shown in Table 1.

3.2 Cell adhesion

Fig. 2 shows cell adhesion on tissue culture plastic (TCP) surfaces at various concentrations (100 nM, 1 μM, 10 μM and 100 μM) of **GP1**, **GP2** and **GP3** in the cell culture media. To carry out quantitative analysis of adhesion % of osteoblast cells, we used colorimetric cell-surface adhesion assay in which cells were incubated with MTT after 4 h of cell adhesion on surface. Non-adhered cells were washed off by removing the culture media. Dimethylsulfoxide was added to the surface adhered cells, and then the absorbance was measured at 595 nm as described previously.[51] This method is well accepted for measuring the number of adherent cells.[64]

The use of **GP1** at various concentrations did not exhibit any significant change on osteoblast cell adhesion. However, the %

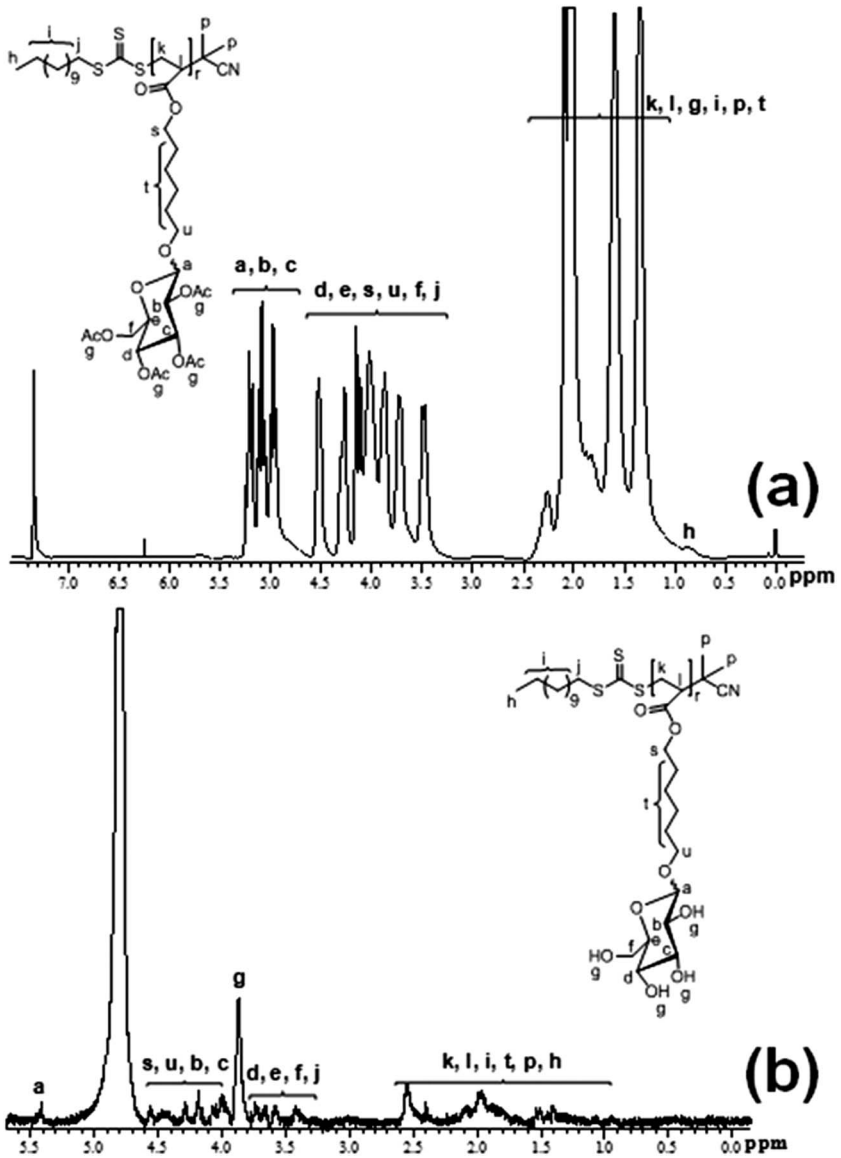

Fig. 1 ^{1}H-NMR spectra of (a) poly(AHTAGP) in $CDCl_3$ and (b) **GP3** in D_2O.

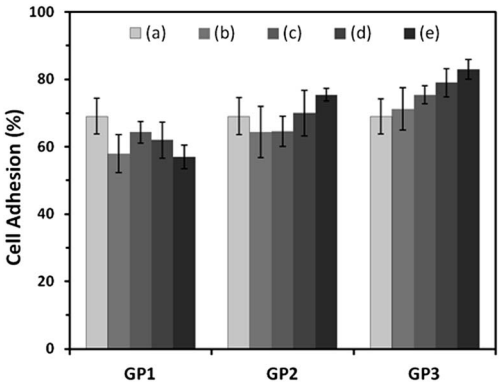

Fig. 2 Osteoblast cell adhesion after 4 h at (a) without the use of glycopolymers, (b) 100 nM, (c) 1 μM, (d) 10 μM and (e) 100 μM of glycopolymers.

of cell adhesion was a little less than the cell adhesion achieved on TCP without the use of **GP1**. The use of **GP3** at 100 μM showed about 6% increase in cell adhesion compared to **GP2**. Fig. 3 shows cell adhesion on TCP surfaces at higher concentrations (10 μM to 2000 μM) of **GP1**, **GP2** and **GP3** and these results were compared to the one without glycopolymers. It has been shown that the use of 10 and 100 μM of **GP1** and **GP2** did not cause any significant change on osteoblast cells adhesion. However, a further increase in the concentration (1000 and 2000 μM) of **GP1** and **GP2** showed a rapid decrease in osteoblast cell adhesion. On the other hand, **GP3**, which has the longest pendant alkyl chain of glucose moiety in glycopolymer we used, showed relatively better osteoblast cell adhesion at concentrations similar to those of **GP1** and **GP2**.

These observations clearly indicate that the decrease in pendant alkyl chain length of glucose moiety in glycopolymer can reduce cell adhesion at higher concentrations. To have a better understanding on the role of pendant alkyl chain length of glucose moiety on osteoblast cells, an estimation of glucose moiety weight percentage (wt%) in each glycopolymer was calculated from ^{1}H NMR (see Experimental, eqn (1) and (2)). The increase in the pendant spacer length (0, 4 and 6 alkyl chain length) of glycopolymer decreased the covalently bonded glucose moiety packing density in glycopolymer (71, 56 and 48 wt%, respectively). Hence, cell adhesion was plotted against covalently bonded glucose moiety concentration in glycopolymers (ESI, Fig. S11†). The **GP1** and **GP2** exhibited similar osteoblast cell adhesion up to 300 μM of covalently bonded glucose moiety and a further increase in concentration showed a decrease in osteoblast cell adhesion. Whereas, **GP3**, which has the longest pendant alkyl chain length of glucose moiety in glycopolymer, showed relatively better osteoblast cell adhesion at similar concentrations of covalently bonded glucose moiety of **GP1** and **GP2**. To further validate the above results, free glucose (**FG**) at various concentrations was added to the culture media, and there was no significant difference on cell adhesion observed with increasing **FG** concentrations (ESI, Fig. S11†).

3.3 Immunofluoresence staining

It is well established that cell spreading and movement occur, although the process of the binding of cell surface integrin receptors to extracellular matrix adhesion molecules. The complex at the focal adhesions consists of several proteins, such as vinculin, talin, α-actin and paxillin, at the intracellular face of the plasma membrane. Thus, for a better understanding on cell adhesion and cytoskeletal organization, integrin α5 and talin co-stained microscopic images of osteoblast cells on plastic tissue culture surfaces of all three glycopolymers at various concentrations were obtained. Talin and integrin α5 immunostaining were performed at 1 μM of **GP1**, **GP2** and **GP3** and cell cytoskeletal organization was compared with control, which was without glycopolymer on plastic tissue culture surfaces, as shown in Fig. 4. From the observations, it was clearly indicative that cell spreading was observed in the presence of different glycopolymers, and the relative number of the focal contact points decreased with an increase in pendant spacer length of glucose moiety in glycopolymers from **GP1** to **GP3**. Merged immunostained images clearly showed that talin co-localized with integrin α5. The integrin α5 staining images showed a functional role of the cytoplasmic domain of the alpha subunit of the integrin, which played an important role in determining cell surface interaction.[65] Optical images of the cells at 1 μM of **GP1**, **GP2** and **GP3** were obtained and are shown in Fig. 5. A decrease in the number of cells was observed with increasing glycopolymers concentrations (ESI, Fig. S12†). To investigate cell motility and cytoskeletal organization at various concentrations of **GP1**, **GP2** and **GP3**, integrin α5 and talin immunostaining were performed and the results are shown in ESI, Fig. S13–15†, respectively. A significant difference was observed at various concentrations of glycopolymer with increasing pendant spacer length of glucose moiety in glycopolymers. **GP2**

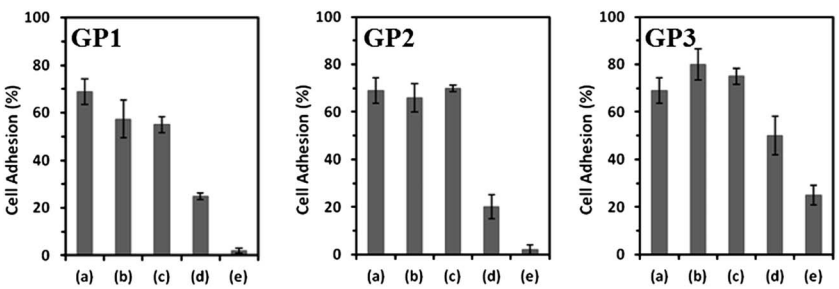

Fig. 3 Osteoblast cell adhesion after 4 h at (a) without the use of glycopolymer, (b) 10, (c) 100, (d) 1000, and (e) 2000 μM of glycopolymers.

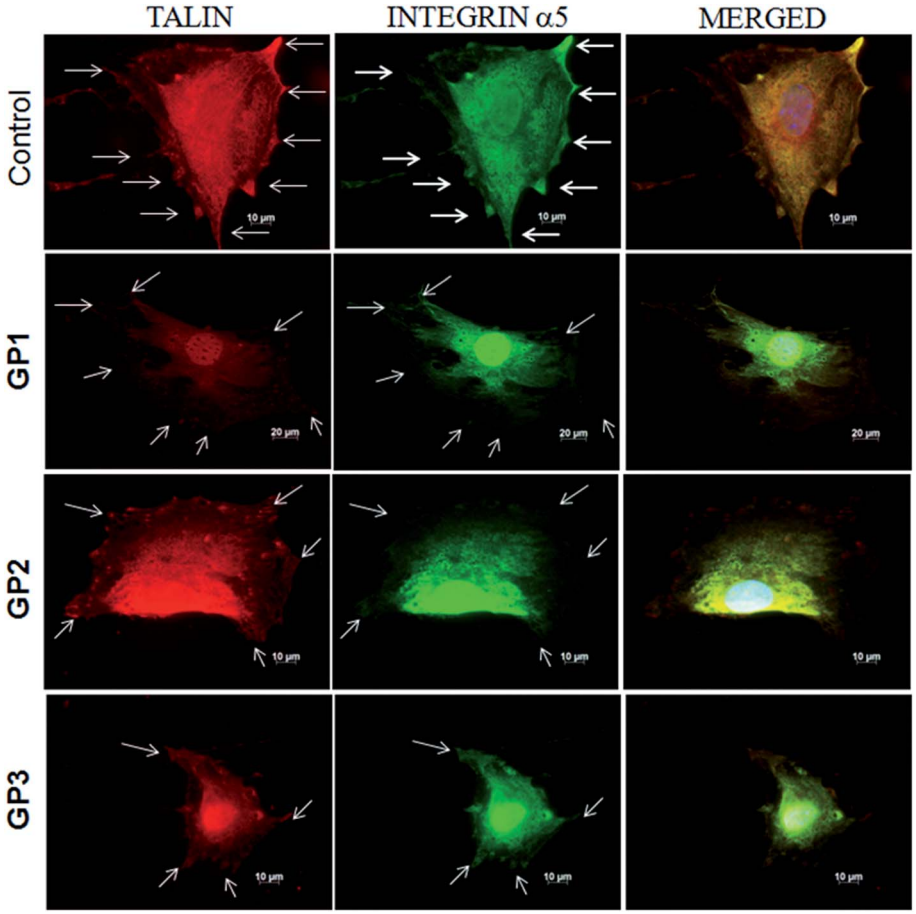

Fig. 4 Fluorescent microscopic images of osteoblast cells stained with integrin α5 and talin at 1 μM of **GP1**, **GP2**, **GP3** and control (without the use of glycopolymer).

(ESI, Fig. S14†) and **GP3** (ESI, Fig. S15†) showed better cell spreading as compared to **GP1** (ESI, Fig. S13†) at similar concentrations.

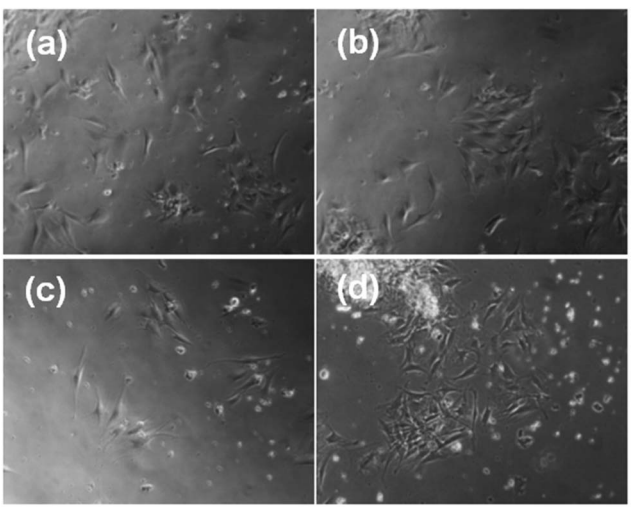

Fig. 5 Brightfield microscopic images of osteoblast cells (a) control (without the use of glycopolymer) and at 1 μM of (b) **GP1**, (c) **GP2** and (d) **GP3**.

Actin staining on TCP was used for the qualitative analysis of cell spreading in terms of cytoskeleton protein expression at various concentrations of **GP1**, **GP2** and **GP3**, and the results are shown in Fig. 6. These observations clearly indicate that the concentration of glycopolymers have effects on cell morphology and spreading. The use of low concentrations (<100 μM) of all three glycopolymers did not result in any observable differences in actin staining, and the results were similar to the staining obtained on TCP without glycopolymers (ESI, Fig. S16†). Concentrations at and above 1000 μM of **GP1** and **GP2** showed reduced focal contact points, which led to a shrinkage in the cell size. Although the obtained microscopic actin stained cell images at higher concentrations (up to 2000 μM) of **GP3** maintained a significantly good number of focal points, no shrinkage in the cell size was observed. Integrin α5 and talin staining on TCP of glycopolymers at higher concentrations were obtained and a significant reduction was observed in cell spreading. Similar results were observed for integrin α5 and talin for the use of glycopolymers at higher concentrations and a representative result of immunostained osteroblast cell at 1000 μM of **GP3** was given in ESI, Fig. S17.†

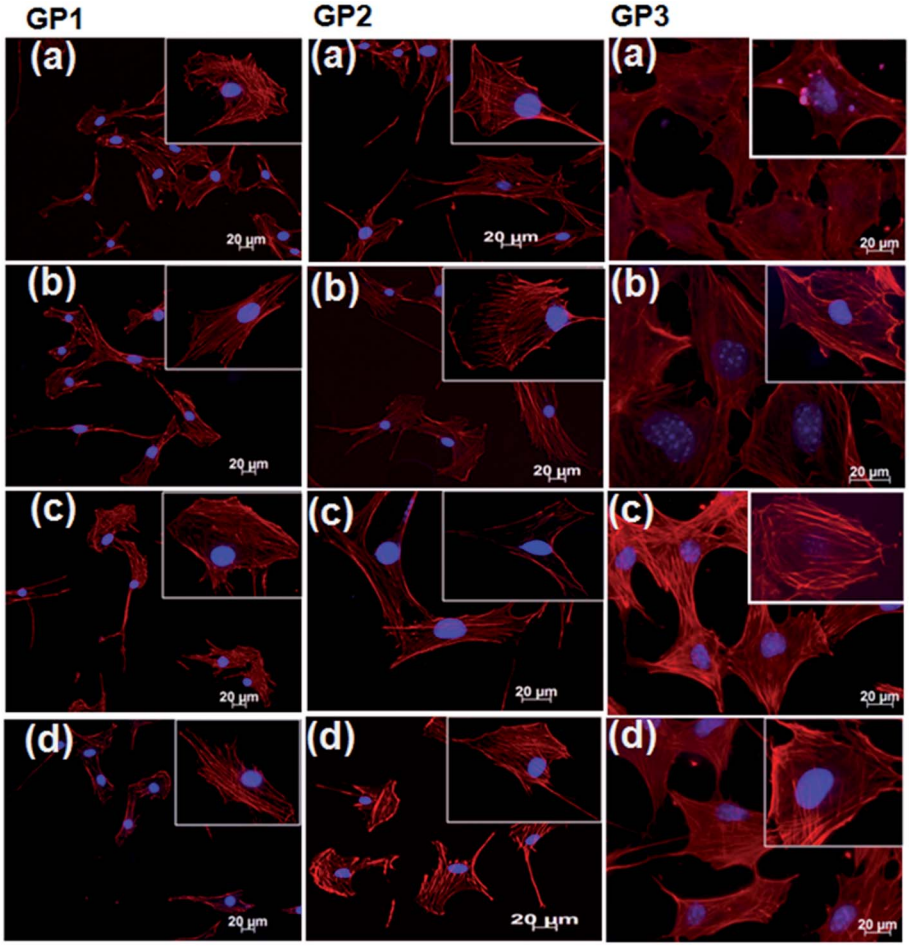

Fig. 6 Fluorescent microscopy images of actin stained osteoblast cells for assessing the expression of cytoskeleton protein at (a) 10, (b) 100, (c) 1000, and (d) 2000 μM of glycopolymers. Insets are magnified images.

3.4 Osteoblast cell viability and proliferation

There was no significant difference in cell viability observed at the lower concentrations of covalently bonded glucose moiety of **GP1** and **GP3** as compared to the cell viability (~70%) without the use of the glycopolymers (Fig. 7). **GP2** showed higher cell viability (~95%) for concentrations up to 300 μM as compared to the cell viability obtained for **GP1** and **GP3**. A further increase (>300 μM) in the concentration of covalently bonded glucose moiety of **GP1** and **GP2** showed a steep decrease in cell viability. However, the use of the **GP3** at

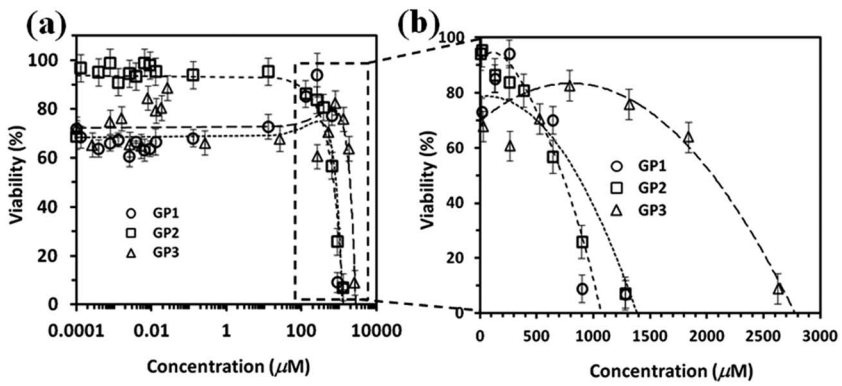

Fig. 7 Osteoblast cell viability after 24 h at various concentrations of covalently bonded glucose moiety in glycopolymers. Cells viability values plotted in (a) logarithmic scale which highlights relatively low concentrations and (b) normal scan which highlights response at higher concentrations. In logarithmic scale the values at 0.0001 represent cell viability without addition of the glycopolymers.

concentrations above 300 μM showed a relatively slow decrease in cell viability. The osteoblast cells were able to maintain their normal viability at higher concentrations (up to 2000 μM) for the use of covalently bonded glucose moiety of **GP3**, the glucose moiety of which has the longest pendant alkyl chain length compared to the **GP1** and **GP2**.

Osteoblast cell proliferation was estimated at 24, 48 and 72 h after plating the cells at various concentrations (0–3000 μM) of covalently bonded glucose moiety of glycopolymers, and the results are shown in Fig. 8. At lower concentrations (0 to 300 μM), the cell proliferation did not exhibit any significant difference with variations in alkyl chain length of glucose moiety in glycopolymers. Cell proliferation was reduced rapidly with a further increase in the concentration of covalently bonded glucose moiety of **GP1** and **GP2** and most of the cells lost their viability at the concentration of 1000 μM. Interestingly, we did not observe any adverse effects on osteoblast cell viability at 2000 μM of covalently bonded glucose moiety of **GP3**.

As per our knowledge and available literature, this is the first report in which the effects of covalently bonded spacer length of glucose in glycopolymer on osteoblast cells have been investigated. However, previous studies have shown the improved cell response on metal surfaces having micro/nano-topography and polymeric scaffolds at *in vitro* and *in vivo* conditions.[66–70] Hence, we expect to use this macromolecular architecture design for developing glycopolymers coatings on metal implants in the future.

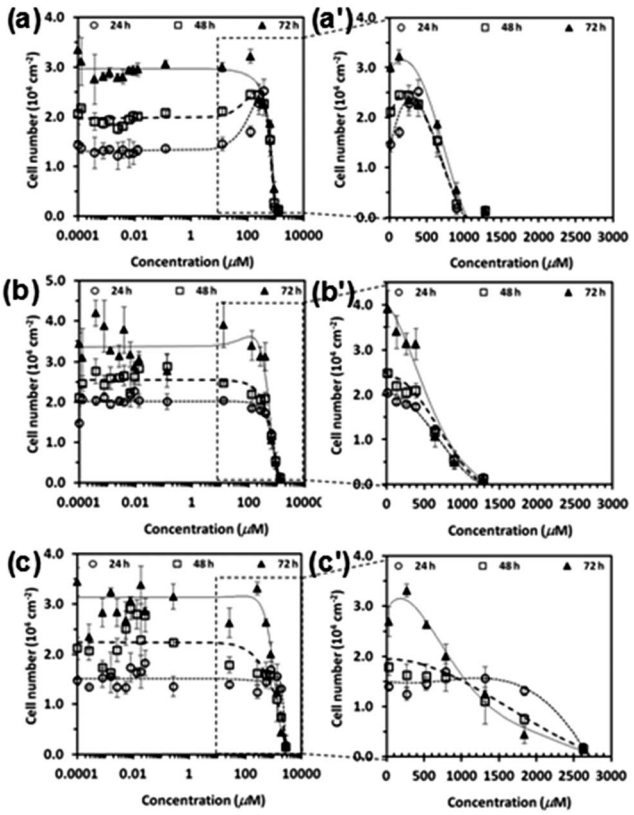

Fig. 8 Osteoblast cell proliferation at various concentrations of covalently bonded glucose moiety of glycopolymers assessed at 24, 48 and 72 h after cell plating. (a) GP1, (b) GP2 and (c) GP3 responses were plotted in logarithmic scale. In logarithmic scale the values at 0.0001 represent cell proliferation without addition of the glycopolymers. (a′) GP1, (b′) GP2 and (c′) GP3 response were plotted in normal scale to highlight variations at higher concentrations.

4. Conclusions

In conclusion, glycopolymers were synthesized by introducing different alkyl chain spacer lengths between glucose moiety and polymer backbone and dodecyl alkyl chain at one terminal end of the macromolecular chain *via* the RAFT process. The effects of pendant spacer lengths of functional moieties in glycopolymers on osteoblast cell adhesion, viability and proliferation were investigated. It was demonstrated that the cytotoxicity limits of osteoblast cells depend on the pendant spacer length of glucose moieties in glycopolymer. Among the synthesized glycopolymers, the glycopolymer with six pendant spacer lengths of glucose moiety exhibited better osteoblast cell adhesion and proliferation at relatively higher concentrations. These glycopolymers may have a potential role in orthopaedic applications as a biologically active coating material on implants.

Acknowledgements

AVSS and MD thank the Council for Scientific and Industrial Research, India, for financial support in network projects CSC 0134 and BSC-0112, respectively. We thank CSIR-CCMB for the microscopy facility. MT, TR and GK thank CSIR, UGC and CSIR network project for providing fellowships, respectively. MD is thankful to Mr N R Chakravarthi, Microscopy Facility of CCMB, for his help in obtaining brightfield images of cells.

References

1 E. Palomino, *Adv. Drug Delivery Rev.*, 1994, **13**, 311–323.
2 X. M. Chen, J. S. Dordick and D. G. Rethwisch, *Macromolecules*, 1995, **28**, 6014–6019.
3 J. Li, S. Zacharek, X. Chen, J. Wang, W. Zhang, A. Janczuk and P. G. Wang, *Bioorg. Med. Chem.*, 1999, **7**, 1549–1558.
4 M. G. Garcia-Martin, C. Jimenez-Hidalgo, S. S. J. Al-Kass, I. Caraballo, M. V. de Paz and J. A. Galbis, *Polymer*, 2000, **41**, 821–826.
5 A. C. Roche, I. Fajac, S. Grosse, N. Frison, C. Rondanino, R. Mayer and M. Monsigny, *Cell. Mol. Life Sci.*, 2003, **60**, 288–297.
6 Y. H. Yun, D. J. Goetz, P. Yellen and W. Chen, *Biomaterials*, 2004, **25**, 147–157.
7 X. Dai, C. Dong and D. Yan, *J. Phys. Chem. B*, 2008, **112**, 3644–3652.
8 A. M. Granville, D. Quémener, T. P. Davis, C. Barner-Kowollik and M. H. Stenzel, *Macromol. Symp.*, 2007, **255**, 81–89.
9 N. Sharon and H. Lis, *Sci. Am.*, 1993, **268**, 82–89.
10 M. Ambrosi, N. R. Cameron and B. G. Davis, *Org. Biomol. Chem.*, 2005, **3**, 1593–1608.
11 H. J. Gabius, H. C. Siebert, S. Andre, J. Jimenez Barbero and H. Rudiger, *ChemBioChem*, 2004, **5**, 740–764.

12 K. H. Mortell, M. Gingras and L. L. Kiessling, *J. Am. Chem. Soc.*, 1994, **116**, 12053–12054.
13 M. Kanai, K. H. Mortell and L. L. Kiessling, *J. Am. Chem. Soc.*, 1997, **119**, 9931–9932.
14 L. L. Kiessling, J. E. Gestwicki and L. E. Strong, *Curr. Opin. Chem. Biol.*, 2000, **4**, 696–703.
15 C. W. Cairo, J. E. Gestwicki, M. Kanai and L. L. Kiessling, *J. Am. Chem. Soc.*, 2002, **124**, 1615–1619.
16 M. Dhayal and D. Ratner, *Langmuir*, 2009, **25**, 2181–2187.
17 G. Wulff, L. Zhu and H. Schmidt, *Macromolecules*, 1997, **30**, 4533–4539.
18 G. Wulff, H. Schmidt and L. Zhu, *Macromol. Chem. Phys.*, 1999, **200**, 774–782.
19 J. Klein, M. Kunz and J. Kowalczyk, *Macromol. Chem. Phys.*, 1990, **191**, 517–528.
20 G. Coullerez, P. H. Seeberger and M. Textor, *Macromol. Biosci.*, 2006, **6**, 634–647.
21 Y. Miura, *J. Polym. Sci., Part A: Polym. Chem.*, 2007, **45**, 5031–5036.
22 V. Ladmiral, E. Melia and D. M. Haddleton, *Eur. Polym. J.*, 2004, **40**, 431–449.
23 R. Pieters, *Med. Res. Rev.*, 2007, **27**, 796–816.
24 L. L. Kiessling and J. C. Grim, *Chem. Soc. Rev.*, 2013, **42**, 4476–4491.
25 V. Ladmiral, E. Melia and D. M. Haddleton, *Eur. Polym. J.*, 2004, **40**, 431–449.
26 M. Ambrosi, N. R. Cameron, B. G. Davis and S. Stolnik, *Org. Biomol. Chem.*, 2005, **3**, 1476–1480.
27 S. G. Spain, M. J. Gibson and N. R. Cameron, *J. Polym. Sci., Part A: Polym. Chem.*, 2007, **45**, 2059–2072.
28 A. J. Varma, J. F. Kennedy and P. Galgali, *Carbohydr. Polym.*, 2004, **56**, 429–445.
29 D. Cunliffe, S. Pennadam and C. Alexander, *Eur. Polym. J.*, 2004, **40**, 5–25.
30 N. Sharon, *Biochim. Biophys. Acta*, 2006, **1760**, 527–537.
31 S. G. Spain and N. R. Cameron, *Polym. Chem.*, 2011, **2**, 60–68.
32 L. L. Kiessling, J. E. Gestwicki and L. E. Strong, *Angew. Chem., Int. Ed.*, 2006, **45**, 2348–2368.
33 T. K. Dam and F. C. Brewer, *Glycobiology*, 2010, **20**, 1061–1064.
34 A. Varki, *Glycobiology*, 1993, **3**, 97–130.
35 R. L. Schnaar, P. H. Weigel, M. S. Kuhlenschmidt, Y. C. Lee and S. Roseman, *J. Biol. Chem.*, 1978, **253**, 7940–7951.
36 S. Muthukrishnan, M. Nitschke, S. Gramm, Z. Ozyurek, B. Voit, C. Werner and A. H. E. Mueller, *Macromol. Biosci.*, 2006, **6**, 658–666.
37 A. T. Gutsche, P. Parsons-Wingerter, D. Chand, W. M. Saltzman and K. W. Leong, *Biotechnol. Bioeng.*, 1994, **43**, 801–809.
38 S.-H. Kim, T. Hoshiba and T. Akaike, *J. Biomed. Mater. Res., Part A*, 2003, **67**, 1351–1359.
39 J.-Y. Wang, F. Xiao, Y.-P. Zhao, L. Chen, R. Zhang and G. Guo, *Carbohydr. Polym.*, 2010, **82**, 578–584.
40 R. L. Schnaar, *Anal. Biochem.*, 1984, **143**, 1–13.
41 J. A. Oka and P. H. Weigel, *J. Cell Biol.*, 1986, **103**, 1055–1060.
42 J. S. Lee, S. H. Kim, Y. J. Kim, T. Akaike and S. C. Kim, *Biomacromolecules*, 2005, **6**, 1906.
43 S. Forster and M. Antonietti, *Adv. Mater.*, 1998, **10**, 195–217.
44 J. Hawker and K. L. Wooley, *Science*, 2005, **309**, 1200–1205.
45 A. Kobayashi, A. Koyama, M. Goto, K. Kobayashi, C.-W. Chang, K. Tomita and T. Akaike, *Proc. Jpn. Acad.*, 1993, **69**, 89–94.
46 K.-H. Park, R. Takei, M. Goto, A. Maruyama, A. Kobayashi, K. Kobayashi and T. Akaike, *J. Biochem.*, 1997, **121**, 997–1001.
47 M. Dhayal, R. Kapoor, P. G. Sistla, R. R. Pandey, S. Kar, K. K. Saini and G. Pande, *Mater. Sci. Eng., C*, 2014, **37**, 99–107.
48 M. Dard, M. A. Sewing, J. Meyer, S. Verrier, S. Roessler and D. Scharnweber, *Clin. Oral Investig.*, 2000, **4**, 126–129.
49 B. Vagaska, L. Bacakova, E. Filova and K. Balik, *Physiol. Res.*, 2010, **59**, 309–322.
50 W. H. Chen, Y. Tabata and Y. W. Tong, *Curr. Pharm. Des.*, 2010, **16**, 2388–2394.
51 M. Dhayal, R. Kapoor, P. G. Sistla, C. Kant, R. R. Pandey, G. Krishnan Kumar Saini and G. Pande, *J. Biomed. Mater. Res., Part A*, 2012, **100**, 1168–1178.
52 K. Anselme, *Biomaterials*, 2000, **21**, 667–681.
53 C. J. Wilson, R. E. Clegg, D. I. Leavesley and M. J. Pearcy, *Tissue Eng., Part A*, 2005, **11**, 1–18.
54 K. C. Dee and R. Bizios, *Biotechnol. Bioeng.*, 1996, **50**, 438–442.
55 K. Babiuch, C. R. Becer, M. Gottschaldt, J. T. Delaney, J. Weisser, B. Beer, R. Wyrwa, M. Schnabelrauch and U. S. Schubert, *Macromol. Biosci.*, 2011, **11**, 535–548.
56 L. A. Hidalgo-Bastida and S. H. Cartmell, *Tissue Eng., Part B*, 2010, **16**, 405–412.
57 A. B. Lowe, B. S. Sumerlin and C. L. McCormick, *Polymer*, 2003, **44**, 6761–6765.
58 L. Albertin, M. Stenzel, C. Barner-Kowollik, L. J. R. Foster and T. P. Davis, *Macromolecules*, 2004, **37**, 7530–7537.
59 N. R. Cameron, S. G. Spain, J. A. Kingham, S. Weck, L. Albertin, C. A. Barker, G. Battaglia, T. Smart and A. Blanazs, *Faraday Discuss.*, 2008, **139**, 359–368.
60 M. Sim, H. Kondo and C. H. Wong, *J. Am. Chem. Soc.*, 1993, **115**, 2260–2267.
61 J. W. Woodcock, X. Jiang, R. A. E. Wright and B. Zhao, *Macromolecules*, 2011, **44**, 5764–5775.
62 Z. Petrovica, S. Konstantinovic and A. Spasojevic, *Indian J. Chem., Sect. B: Org. Chem. Incl. Med. Chem.*, 2004, 132–134.
63 G. Pasparakis and C. Alexander, *Angew. Chem., Int. Ed.*, 2008, **47**, 4847–4850.
64 I. Miki, N. Ishihara, M. Otoshi and H. Kase, *J. Immunol. Methods*, 1993, **164**, 255–261.
65 J. S. Bauer, J. Varner, C. Schreiner, L. Kornberg, R. Nicholas and R. L. Juliano, *J. Cell Biol.*, 1993, **122**, 209–221.
66 H. Nathaniel and D. J. Mooney, *Nature*, 2009, **462**, 426–432.
67 M. P. Lutolf, F. E. Weber, H. G. Schmoekel, J. C. Schense, T. Kohler, R. Muller and J. A. Hubbell, *Nat. Biotechnol.*, 2003, **21**, 513–518.
68 J. A. Hubbell, *Nat. Biotechnol.*, 1995, **13**, 565–576.
69 Z. You, H. Cao, J. Gao, P. H. Shin, B. W. Day and Y. Wang, *Biomaterials*, 2010, **31**, 3129–3138.
70 Y. Miura, *Polym. J.*, 2012, **44**, 679–689.

